

- (32) Lindman, B.; Forsén, S.; Forslind, E. *J. Phys. Chem.* **1968**, *72*, 2805.  
 (33) Wennerström, H.; Lindman, B.; Forsén, S. *J. Phys. Chem.* **1971**, *75*, 2936.  
 (34) Hertz, H. G.; Holz, M. *J. Phys. Chem.* **1974**, *78*, 1002.  
 (35) Feil, D.; Jeffrey, G. A. *J. Chem. Phys.* **1961**, *35*, 1863.  
 (36) Pedersen, C. J. *J. Am. Chem. Soc.* **1967**, *89*, 7017.  
 (37) Truter, M. R. *Struct. Bonding (Berlin)* **1973**, *16*, 71.  
 (38) Izatt, R. M.; Eatough, D. J.; Christensen, J. J. *Struct. Bonding (Berlin)* **1973**, *16*, 161.  
 (39) Lin, J. D.; Popov, A. I. *J. Am. Chem. Soc.* **1981**, *103*, 3773.  
 (40) Grandjean, J.; Laszlo, P.; Offerman, W.; Rinaldi, P. *J. Am. Chem. Soc.* **1981**, *103*, 1380.  
 (41) Vögtle, F.; Weber, E. *Angew. Chem., Int. Ed. Engl.* **1979**, *18*, 753.  
 (42) Shchori, E.; Jagur-Grodzinski, J.; Luz, Z.; Shporer, M. *J. Am. Chem. Soc.* **1971**, *93*, 7133.  
 (43) Eisenstadt, M.; Friedman, H. L. *J. Chem. Phys.* **1966**, *44*, 1407.  
 (44) Hall, C.; Richards, R. E.; Schulz, G. N.; Sharp, R. R. *Mol. Phys.* **1969**, *16*, 529.

## Molecular Mechanism of the Ring-Flip Process in Polycarbonate

Jacob Schaefer\* and E. O. Stejskal

Physical Sciences Center, Monsanto Company, St. Louis, Missouri 63167

Dennis Perchak,<sup>†</sup> Jeffrey Skolnick,<sup>‡</sup> and Robert Yaris

Department of Chemistry, Washington University, St. Louis, Missouri 63130

**ABSTRACT:** Calculations of the conformational preferences of isolated single chains of poly(2,6-dimethylphenylene oxide) (PPO) and bisphenol-A polycarbonate (PC) predict that the rings of both chains are nearly free rotors at room temperature. However, experimental dipolar rotational spin-echo <sup>13</sup>C NMR shows that in the glass, the rings of PPO execute only small-amplitude motions while those of PC undergo primarily 180° ring flips (a hindered rotation) superimposed on some wiggles. Geometrical considerations of the dense packing of chains in the glass suggest that the rings of adjacent chains block rotational freedom. We propose that the mobility of the PC main chain results in lattice distortions which allow ring flips not permitted by the stiffer PPO main chain.

### Introduction

Polycarbonates undergo a variety of large-amplitude molecular motions, some of which have been characterized recently by the collapse of deuterium quadrupolar,<sup>1</sup> carbon chemical shift,<sup>2</sup> and dipolar<sup>3</sup> tensors. The dominant motion for bisphenol-A polycarbonate (PC) is 180° flips about the aromatic-ring C<sub>2</sub> symmetry axis. These flips occur over a broad range of frequencies centered about 300 kHz at room temperature. The flips are superimposed on 30° ring oscillations about the same axis. Other main-chain motions are also significant; amplitudes of these wiggling motions are of the order of 20° (root mean square).<sup>3</sup>

In this paper we demonstrate experimentally that poly(2,6-dimethylphenylene oxide) (PPO) and its methyl-brominated analogue have no large-amplitude motions in the glass at room temperature. We then relate the differences between microscopic molecular motions in PC and PPO to the differences in their anelastic mechanical loss behavior. This connection aids in the identification of a mechanically active lattice distortion in PC which we claim is ultimately responsible for its ring flips.

### Experiments

Carbon dipolar tensors were characterized by using dipolar rotational spin-echo <sup>13</sup>C NMR at 15.1 MHz with magic-angle spinning,<sup>4</sup> usually at 1894 Hz. This is a two-dimensional experiment in which, during the additional time dimension, carbon magnetization is allowed to evolve under the influence of C-H coupling while H-H coupling is suppressed by homonuclear multiple-pulse (WAHUA) decoupling.<sup>5,6</sup> For singly protonated carbons whose resonances are well resolved in the chemical shift dimension, a Fourier transform of the intensity at the peak maximum vs. evolution time yields a dipolar spectrum<sup>3</sup> consisting of a <sup>13</sup>C-<sup>1</sup>H Pake doublet, scaled by the WAHUA decoupling, and broken up into sidebands by the magic-angle spinning.<sup>7</sup>

Molecular motion modifies this pattern just as it does quadrupolar line shapes.<sup>1,3</sup>

Carbon dipolar tensor simulations were performed by using the methods developed by Herzfeld and Berger.<sup>8</sup> Calculations of tensors partially collapsed by restricted molecular motion were performed by assuming the motion was fast compared to the dipolar interactions. Formulas for tensor components under various types of restricted motions (and compatible with the Herzfeld and Berger analysis) are given in the appendix to ref 3.

Polycarbonate and tetrachloropolycarbonate were examined as annealed molded glasses, and the two PPOs as precipitated powders.

Conformational maps were calculated by modeling the benzene-benzene interaction potential using the Gaussian overlap procedure due to Berne and Pechukas.<sup>9</sup> This model treats phenyl rings as ellipsoids of revolution. The potential is proportional to the amount of overlap of the ellipsoids, with bond-angle bending or stretching not included. The overlap model yields orientation-dependent range and strength parameters which are used in conjunction with a 12-6 Lennard-Jones potential. The overlap model thus reduces the calculation of the benzene-benzene interaction from a large sum of atomic site-site terms to a single two-body term with a distance and orientation dependence. The overlap model is also used for isotropic molecules, which are treated as spheres. In producing conformational maps for both polycarbonate and poly(phenylene oxide), oblate ellipsoids were used for the rings, and spheres for the methyl groups.

### Results

Dipolar rotational spin-echo <sup>13</sup>C NMR spectra of a methyl-brominated version of PPO are shown in Figure 1. The resonances of the protonated aromatic carbons (115 ppm) and the methylene carbons (25 ppm) rapidly dephase after as little as two WAHUA cycles. The nonprotonated aromatic-carbon signals (130-160 ppm) are not strongly influenced by proton coupling and experience little dephasing. The methyl-carbon signal (15 ppm) is intermediate in behavior.

All the carbon resonances refocus after 16 cycles. The rotation period for the magic-angle spinning was chosen

<sup>†</sup> Present address: Department of Macromolecular Science, Case Western Reserve University, Cleveland, OH 44106.

<sup>‡</sup> A. P. Sloan Foundation Fellow.

Table I  
Carbon-13 Relaxation Parameters for Some Polycarbonates and Poly(phenylene oxides)

polymer	$\langle T_{1\rho}(C) \rangle$ , ms ( $H_1(C) = 44$ kHz)		$n_2/n_1$ , aromatic dipolar sideband ratio (MAS = 1894 Hz)	$n_2/n_1$ , methyl dipolar sideband ratio (MAS = 947 Hz)
	aromatic	methyl		
	8	20	0.47	0.57
	140	50	1.52	0.72
	80	200	1.55	0.72
	165	165	1.50	0.79

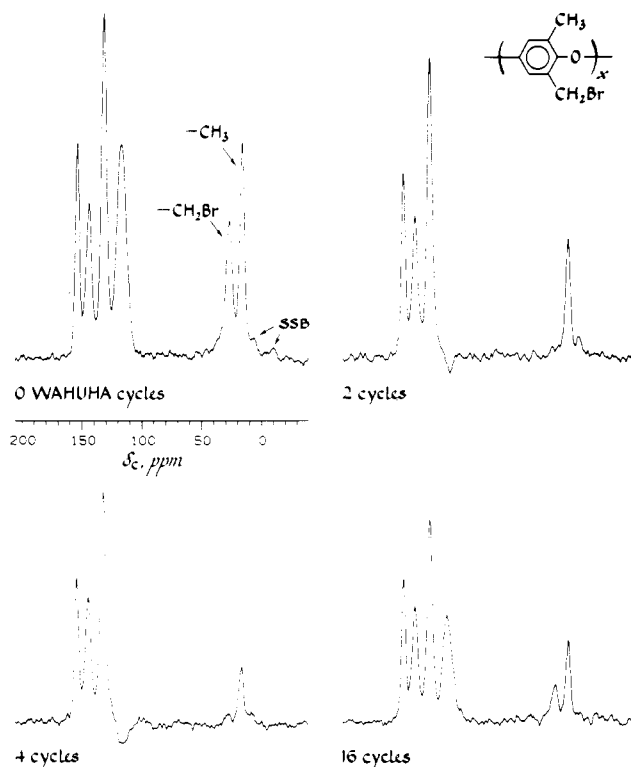


Figure 1. Dipolar rotational spin-echo 15.1-MHz  $^{13}\text{C}$  NMR spectra of a methyl-brominated poly(phenylene oxide) as a function of the number of WAHUA cycles used during  $^1\text{H}$ - $^{13}\text{C}$  dipolar evolution.

so that 16 WAHUA cycles fit in one rotor period. After one rotor revolution, all CH vectors have been restored to the orientations they had following the end of the matched, spin-lock, cross-polarization preparation of the carbon magnetization. Thus, all dephasing of carbon magnetization due to CH coupling has been reversed and a dipolar echo results. The intensity of this echo should match that of the signal before any dephasing (zero WAHUA cycles). The observed echo is only about half as big with losses due primarily to imperfect H-H decoupling.

Dipolar sideband patterns for the CH and  $\text{CH}_3$  groups in the methyl-brominated PPO, in PPO itself, and in a crystalline model compound for PPO, dimethoxybenzene, are shown in Figure 2. The aromatic-carbon dipolar

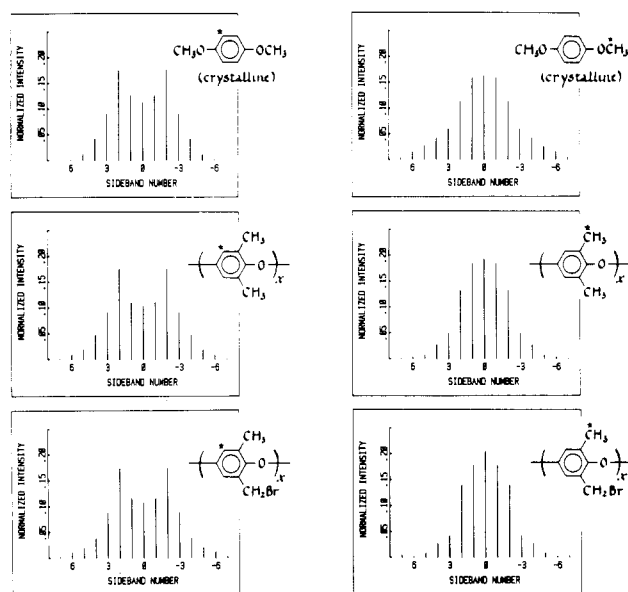


Figure 2. Dipolar Pake patterns for the aromatic CH and methyl  $\text{CH}_3$  for dimethoxybenzene (top), poly(phenylene oxide) (middle), and methyl-brominated poly(phenylene oxide) (bottom). These patterns are the result of 16-point Fourier transforms of absorption-mode data, examples of which are shown in Figure 1. Magic-angle spinning was at 1894 Hz for the patterns on the left and 947 Hz for those on the right.

spectra on the left are all Pake doublets broken up into spinning sidebands separated by 1.894 kHz (the inverse of 16 times the WAHUA cycle time). Each sideband is represented by a single point in the dipolar frequency dimension. Intensities of the sidebands can be reliably compared so long as sideband widths are all equal, an assumption we will make here.

The fact that the PPO and methyl-brominated PPO protonated aromatic-carbon dipolar pattern are indistinguishable from that of a nominally<sup>4</sup> rigid crystalline material (Figure 2, left) means the rings in the two PPOs have no large-amplitude motions. This conclusion is supported by the similarity of the methyl-carbon dipolar patterns for PPO, the methyl-brominated PPO, and dimethoxybenzene (Figure 2, right).

PPO and methyl-brominated PPO have few low-frequency small-amplitude wiggles. Both protonated-aromatic and methyl-carbon  $T_{1\rho}$ 's are an order of magnitude

**Table II**  
**Dipolar Rotational Sideband Intensities for a CH Pair Undergoing Molecular Motion and Magic-Angle Spinning at 1894 Hz**

expt or motional model	sideband no.					
	0	1	2	3	4	5
expt (polycarbonate)	0.247	0.214	0.101	0.037	0.013	0.007
static	0.120	0.124	0.185	0.075	0.038	0.013
180° flips	0.217	0.235	0.111	0.036	0.008	0.002
half static and half flips <sup>a</sup>	0.169	0.180	0.148	0.056	0.023	0.008
wiggles (15° rms CH reorientation on a 120° cone)	0.126	0.136	0.184	0.069	0.033	0.011
half wiggles and half flips <sup>b</sup> + wiggles	0.198	0.188	0.140	0.048	0.019	0.006
flips <sup>b</sup> + wiggles	0.269	0.235	0.095	0.026	0.005	0.001

<sup>a</sup>This designation means half the rings in the sample are static and the other half are undergoing 180° flips. <sup>b</sup>Exact 180° flips independent of the random wiggles.

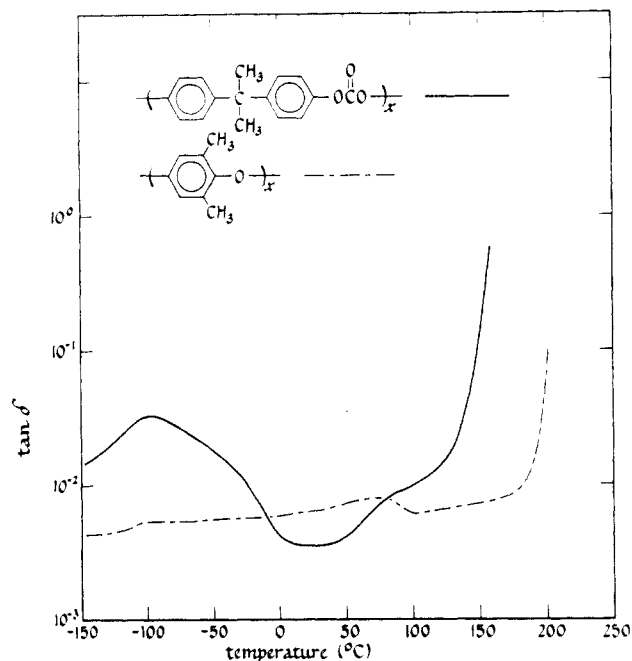


**Figure 3.** Anelastic mechanical shear loss spectra of polycarbonate and poly(phenylene oxide) taken from the work of Yee.<sup>9,10</sup>

longer than those of PC at 44 kHz (Table I). In fact, the PPO relaxation times are comparable to those of a ring-substituted chloro polycarbonate, the rigidity of whose ring and main chain are documented by dipolar sideband intensity ratios comparable to those of crystalline materials (Table I).

With neither large- nor small-amplitude ring motions active at room temperature, it is not surprising the anelastic mechanical loss spectrum of PPO is featureless<sup>10</sup> (Figure 3). By contrast, the PC loss spectrum<sup>11</sup> shows a broad intense peak, centered near -100 °C (at 1 Hz). The activation energy associated with this loss peak is of the order of 10 kcal/mol,<sup>11</sup> which translates to a frequency of about 200 kHz at room temperature, the same average frequency as that of the ring flips.<sup>3</sup>

PC has large-amplitude ring motions which significantly change its sideband pattern from that expected for a static system (Table II, rows 1 and 2). The form of the collapse of chemical shift tensors has been used to prove that the large-amplitude motion predominantly involves 180° flips.<sup>2,3</sup> To match the observed dipolar sideband intensities requires all the rings to flip (Table II, comparisons of rows 1, 4, 6, and 7). This means there is only one dynamic ring population at room temperature, not one undergoing flips and another static.

Even using a carbon rotating-frame spin lock for 20 ms as part of the carbon spin-system preparation prior to the dipolar evolution period reveals no differences in dipolar

**Table III**  
**Ratio of Intensities of Second to First Aromatic CH Dipolar Rotational Sidebands with MAS = 1894 Hz**

<sup>13</sup> C rotating frame spin lock, <sup>a</sup> ms	$n_2/n_1$	
	polycarbonate	poly(BPA-formal) <sup>b</sup>
0.05	0.47	0.75
3.00	0.44	0.87
8.00	0.47	0.95
16.00	0.44	1.06
20.00	0.45	1.28

<sup>a</sup>50% of the protonated-aromatic carbon magnetization decayed after 20 ms with  $H_1(C) = 60$  kHz. <sup>b</sup>Annealed material; ref 3.

patterns between those rings with slow and those with fast rotating-frame relaxation (Table III, middle column). Such differences are readily apparent in polycarbonate-like polymers with multiple populations (Table III, right column).

The flexibility of the polycarbonate main chain can be inferred either from the short methyl-carbon  $T_{1\rho}$  or from the methyl-carbon  $n_2/n_1$  dipolar sideband intensity ratio (Table I). The latter is significantly less than that of either of the PPOs or of tetrachloropolycarbonate (Table I). Both PC parameters are unaffected by ring motions but are direct measures of main-chain wiggling. The weak  $H_1(C)$  dependence<sup>3</sup> of the methyl-carbon  $T_{1\rho}$  means the frequency of the main-chain wiggling is of the order of 100 kHz. This result may explain the inability of deuterium spin alignment experiments to detect main-chain motion.<sup>1</sup> Such experiments are insensitive to motions with correlation times between 10 and 100  $\mu$ s. In addition, the relatively small difference between the observed methyl-carbon  $n_2/n_1$  ratio and the rigid-lattice value suggests a weak temperature dependence for the deuterium quadrupolar splitting of methyl-deuterated polycarbonates. This is especially true in view of the broadly distributed motions characteristic of PC. A 7% decrease in quadrupolar splitting has been observed by Smith<sup>12</sup> between +100 and -100 °C. Smith compared splittings from spectra taken at 10 °C intervals over the entire temperature range to confirm this weak dependence.

## Discussion

**Molecular Motion in PC and PPO.** We begin with a summary of the features of the molecular motion in PC and PPO that any successful model of the dynamics must encompass.<sup>1-3</sup> Polycarbonate undergoes 30° ring oscillations over a broad frequency range plus 180° ring flips between apparent rotational potential minima, with an average flipping rate greater than 100 kHz. The dipolar spinning sideband patterns are inconsistent with a 180° ring flip plus any small-angle oscillation that permits ratcheting around the  $C_2$  aromatic axis and produces motion equivalent to that of a free rotor. On the NMR time scale there is only a single dynamic population at

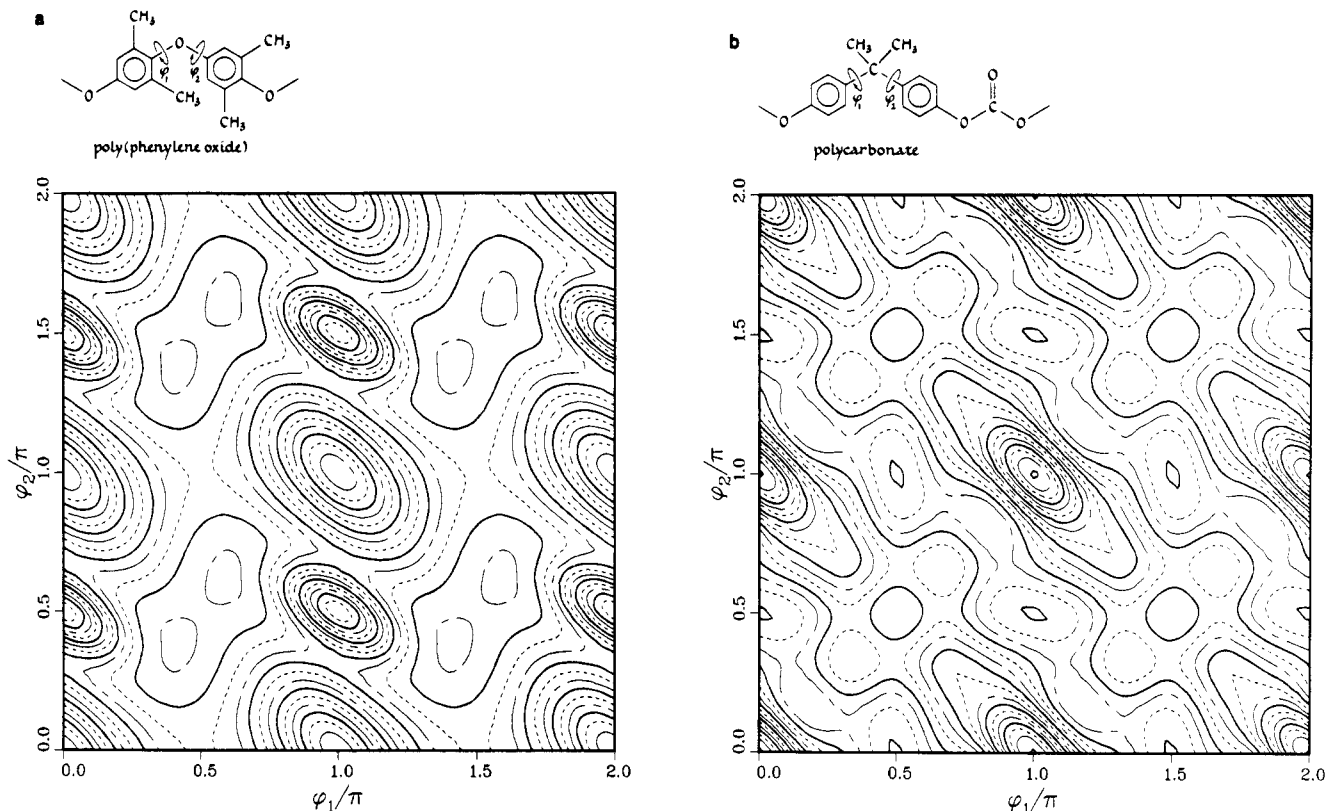


**Figure 4.** Calculated conformational preference maps for poly(phenylene oxide) (left) and polycarbonate (right). The maps were produced by rotating the chain rigidly about the angles  $\phi_1$  and  $\phi_2$  and evaluating the relative potential due to intramolecular interactions. Energy maxima occur in both maps near  $\phi_1 = \phi_2 = 180^\circ$ . An energy minimum exists for poly(phenylene oxide) with  $\phi_1 = \phi_2$  and each slightly displaced from  $\pi/2$ , while a minimum exists for polycarbonate with  $\phi_1 = \pi$  and  $\phi_2 = \pi/2$ . Contours decreasing in relative energy are represented by the sequence solid line, dashed line, dotted line, and increasing in energy by the reverse sequence.

room temperature. If more than one ring population exists, it must interconvert at a rate substantially greater than 100 kHz. Superimposed on ring flips and oscillations are main-chain wiggles indicating that the PC main chain is flexible in the glass. Finally, PC has a broad mechanical loss peak consistent with 200-kHz motion at room temperature, the same frequency regime as the ring flipping. The mechanical loss necessarily involves cooperative motion of the rings.<sup>11</sup> For PPO, there are no large-amplitude motions such as ring flips, and few low-frequency, small-amplitude wiggles. Furthermore PPO possesses a featureless low-temperature mechanical loss spectrum.

**Intramolecular Potential.** Tonelli<sup>13</sup> has calculated the conformational preferences for isolated PC and PPO chains and found the rings in both cases are essentially free rotors at room temperature. We have confirmed these predictions using a calculational approach based on a Gaussian overlap model,<sup>9</sup> with range and strength parameters chosen to match Tonelli's calculated energy minima. Conformational energy maps for both PPO and PC are shown in Figure 4 at higher resolution than those calculated by Tonelli. The rings in both polymers have little difficulty in executing motions about the  $C_2$  axis, with only a few special conformations on these maps forbidden by steric interactions. If  $\phi_1$  in PPO or in PC is set equal to  $90^\circ$ , then Figure 4 shows a broad flat valley with low peaks and shallow valleys for full rotation about  $\phi_2$ . This motion about  $\phi_2$  is essentially free. As shown by Tonelli,<sup>13</sup> the absolute barriers are only of the order of 1–2 kcal/mol. This is not the situation if  $\phi_2$  is fixed near  $0^\circ$  (or  $180^\circ$ ) and  $\phi_1$  varied. There is a sizable steric repulsion between  $\text{CH}_3$  (H) and H (H) groups in PPO (PC) when  $\phi_1$  and  $\phi_2$  are each near  $n \times 180^\circ$ . Hence, the two phenyl rings in adjacent monomer units in PPO, and within a monomer unit

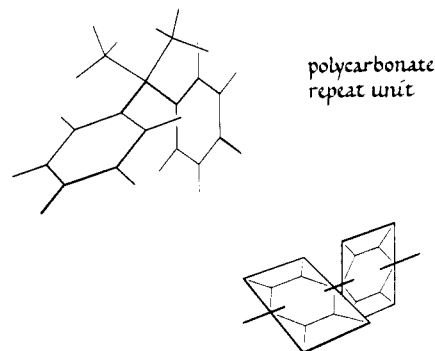


**Figure 5.** Stylized representation of the orthogonal conformational preference of the two rings in the polycarbonate repeat unit.

of PC, are not strictly equivalent. Depending on orientation, constraints can be imagined such that one of the rings can undergo free rotation and the other cannot. However, if the rings rotate cooperatively, they can both behave as free rotors.

Vacuum rotational potentials are useful in that motions which are strongly prohibited (due to steric effects) in the absence of chain-chain interactions will remain prohibited when intermolecular interactions are turned on. However, such a potential energy surface provides no clue as to what additional motions are prohibited when chain-chain packing is taken into account.

**Packing in the Glass.** We know from the experimental dipolar sideband patterns that the rings in PC and PPO in the glass are not free rotors. The deficiency in the potential energy maps of Figure 4 is a result of the omission of the effects of packing in the solid state. If we represent the two rings of the repeat unit of PC (with their slight

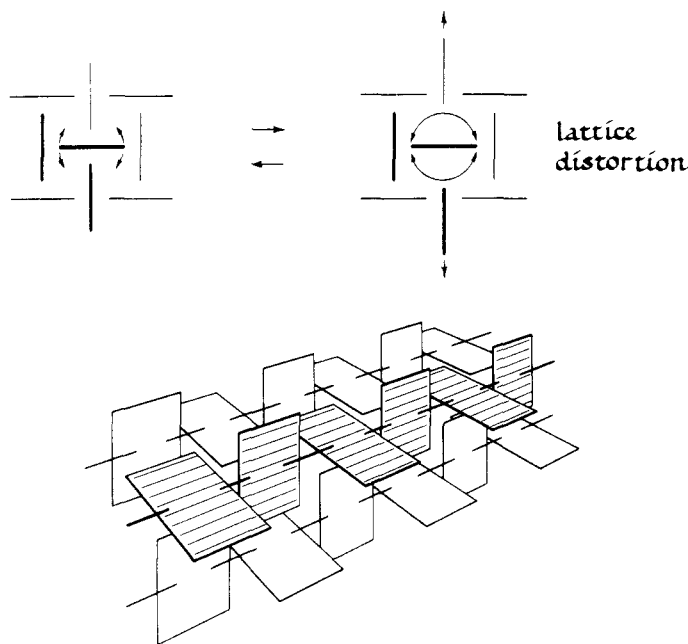


**Figure 6.** Stylized representation of the packing of a few polycarbonate chains in the solid (bottom). Rotational freedom of the rings is limited by interchain steric interactions. A cross section taken perpendicular to the chain bundle axis is shown in the insert (upper left). Rings from chains not shown in the perspective drawing are represented by thinner lines in the insert. When the lattice distorts, rings can rotate until the distortion ends and the rings find themselves in their original position  $\pm n \times 180^\circ$ .

intraunit preference for an orthogonal configuration) by a stylized pair of rectangles (Figure 5), then some appreciation for the influence of packing is possible from a simple perspective drawing of a few chains in the solid (Figure 6). Naturally, we realize PC is not the highly organized polymer suggested by Figure 6. The glass has no long-range order. Nevertheless, local parallelization of chains over a few monomer repeat units occurs even in solutions of long-chain molecules.<sup>14</sup> Our representation is meant to extend over just this sort of short range. For convenience, we have represented all the pairs of rings in PC as rigorously orthogonal, as they are in crystalline bisphenol-A,<sup>3</sup> but this assumption is not a crucial ingredient in the subsequent discussion.

The rings in the PC glass are not free rotors because of the steric constraints imposed by neighboring chains. Ring flips are a hindered motion allowed by the intermolecular constraints. Suppose we assume that the rings are allowed to flip because random packing creates "holes" within which rings are less burdened by steric interactions. These static holes might be interspersed throughout the glass allowing some fraction of the rings freedom. The holes would presumably be big enough to allow a monomer-unit pair to move together to avoid intrachain prohibited conformations.

This static description of the glass is not, however, consistent with all the facts. First, a static-hole description of the ring motion in PC predicts two classes of dynamic rings in PC: those that move in the holes, and those that form the holes. Experiment shows only one population (Tables II and III). If we insist that all the rings are part of the hole boundaries as well as move in them, we are faced with the dilemma of a rather airy structure for PC not at all consistent with the notion of a glass with a density close to that of crystalline material.<sup>15</sup>

In addition, a ring-flip mechanism which involved static holes formed by neighboring chains could yield only a weak

mechanical loss peak. Without distortion or dilation of the lattice, mechanical energy cannot be dissipated by internal frictional losses. In fact, using a dynamic Poisson ratio experiment, Yee<sup>16</sup> has shown that both shear and bulk low-temperature loss peaks occur in PC. Assignment of the ring flips to static holes would therefore lead to the implausible situation that the only large-amplitude motion in PC (and a motion not available to PPO) could not be associated with the low-temperature loss peak which so clearly distinguishes PC from PPO (Figure 3).

**No Wiggles, No Flips.** Instead, we propose a dynamic description of the lattice during the flip process. Rings are indeed constrained from large-amplitude excursions by the rings of neighboring chains. When lattice distortions occur, these constraints are relaxed (Figure 6, top). As the lattice closes up, the rings must either return to their original orientation or have flipped by  $180^\circ$  since these are the only orientations which do not require a lattice distortion. The mechanism of the lattice distortion may include motions such as synchronous rotation<sup>11</sup> or cis/trans isomerization about the carbonate linkage,<sup>17</sup> as well as torsional oscillations. Eventually, all rings participate in both flipping and blocking as lattice breathing moves up and down the chain. The rate of flipping varies across the sample due to local variations in packing. The flip marks an important volume or shape change in the glass, and so flags a mechanically active process. PC rings can flip and PPO rings cannot because of the inherent differences in the mobilities of their lattices.

This description of ring flips in polycarbonate is similar to that proposed by McCammon et al. for tyrosine-ring flips in bovine pancreatic trypsin inhibitor.<sup>18</sup> For this protein, computer simulations of molecular dynamics show that ring flips are occasionally gated on by cooperative displacements of nearby groups. The displacements create local cavities or defects in the protein interior, and these lattice distortions are sufficient to permit ring flips. The complete ring-flip process (rings plus lattice) is a restricted motion, but the flip part of the process need not be. During the picosecond<sup>18</sup> (or fraction of a nanosecond) the ring takes to flip, it is almost a free rotor. This motion is too fast to lead to significant NMR relaxation. Most of the time the ring is clamped undergoing only small-amplitude wiggles. Thus, the time important for NMR relaxation due to flipping is the period between flips. This period is the same for both ring and lattice and leads to  $T_1$  and  $T_{1\rho}$  as a function of  $H_0$  and  $H_1$ , respectively, which are comparable for both ring and main chain.<sup>3</sup>

When the lattice distorts, the ring can flip. When the lattice closes again the ring assumes the original position  $\pm n \times 180^\circ$ . The flip is viewed as an *exact*  $180^\circ$  flip which occurs in mid-wiggle without interrupting the course of the wiggle (Figure 7). The wiggle is the result of cooperative motion of another kind. The flips of Table II are exact  $180^\circ$  flips. If wiggles could continue during the flips (Figure 7, bottom), the combination would result in averaging close to that of a free rotor.<sup>3</sup>

**Cooperative Flips and Mechanical Properties.** We do not know the correlation range of the ring-flip process in PC. Flipping must involve at least two rings down the chain and four or five other rings on other chains. The cooperativity could involve much more.<sup>15</sup> On the other hand, it is also possible that once the lattice distorts, independent wiggles and flips are superimposed on the cooperative flips. Only some of the ring motion need be cooperative.<sup>3</sup>

What we have attempted in this paper is a *description* of the salient features of the ring-flip mechanism in PC:

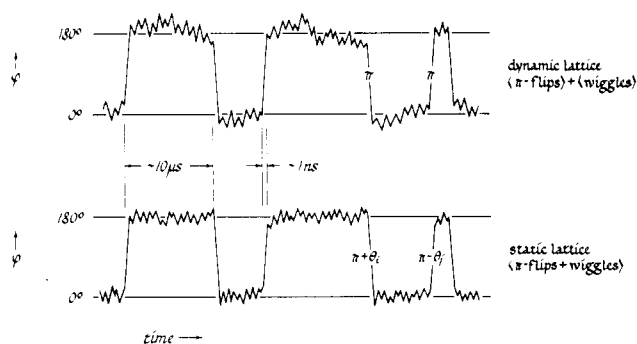


**Figure 7.** Angular excursions for polycarbonate rings under two assumptions for the combination of  $180^\circ$  flips and small-amplitude wiggles. The time for an individual flip may be as short as 1 ps. Many flips can therefore occur in a fraction of a nanosecond. (Only single flips are shown in the figure.) While the total of all elapsed time a ring spends in flipping is small (as established by the experimental dipolar tensors), the time between episodes of flipping must still be short compared to the inverse of C-H dipolar coupling.

the inherent mobility of isolated rings, the constraints produced by packing in the glass, and the cooperative lattice distortion which allows large-amplitude ring motion. We have not attempted an *explanation* of the ring-flip mechanism in terms of activation volumes or monomer-packing symmetry. This requires new experiments to measure directly the motional correlations of rings and, more importantly, a new understanding of the packing interactions in the glass, a development which we feel must await advances in computer modeling of the disordered solid state.

Nevertheless, we can speculate that the presence in PC of a high degree of cooperativity between and along chains in 100-kHz large-amplitude microscopic molecular motions and the unusually high impact strength of PC (its ability to respond to sudden and intense local strains) is no accident. Although impact strength relies ultimately upon

irreversible deformations which we do not measure by either NMR or mechanical loss spectroscopy, if a glass has the ability to respond quickly by the cooperative motion of several chains, it seems reasonable to suppose that many chains can move together in a macroscopic response. Naturally, other factors may intervene and some polymers which show no cooperative motions under low-strain conditions may still respond under high-strain fields.

**Acknowledgment.** This work was supported in part by grants from the National Science Foundation Polymers Program and the Petroleum Research Fund, administered by the American Chemical Society.

**Registry No.** PPO (SRU), 24938-67-8; PC (SRU), 24936-68-3; PPO (polymer), 25134-01-4; PC (polymer), 25037-45-0.

## References and Notes

- (1) Spiess, H. W. *Colloid Polym. Sci.* **1983**, *261*, 193.
- (2) Ingfield, P. T.; Amici, R. M.; Hung, C.-C.; O'Gara, J. F.; Jones, A. A. *Macromolecules* **1983**, *16*, 1552.
- (3) Schaefer, J.; Stejskal, E. O.; McKay, R. A.; Dixon, W. T. *Macromolecules* **1984**, *17*, 1479.
- (4) Schaefer, J.; McKay, R. A.; Stejskal, E. O.; Dixon, W. T. *J. Magn. Reson.* **1983**, *52*, 123.
- (5) Hester, R. K.; Ackerman, J. L.; Neff, B. L.; Waugh, J. S. *Phys. Rev. Lett.* **1976**, *36*, 1081.
- (6) Stoll, M. E.; Vega, A. J.; Vaughan, R. W. *J. Chem. Phys.* **1976**, *65*, 4093.
- (7) Munowitz, M. G.; Griffin, R. G. *J. Chem. Phys.* **1982**, *76*, 2848.
- (8) Herzfeld, J.; Berger, A. E. *J. Chem. Phys.* **1980**, *73*, 6021.
- (9) Berne, B. J.; Pechukas, P. *J. Chem. Phys.* **1971**, *56*, 4213.
- (10) Yee, A. F. *Polym. Eng. Sci.* **1977**, *17*, 213.
- (11) Yee, A. F.; Smith, S. A. *Macromolecules* **1981**, *14*, 54.
- (12) Bubeck, R. A.; Bales, S. E.; Smith, P. *Bull. Am. Phys. Soc.* **1984**, *29*, JT8.
- (13) Tonelli, A. E. *Macromolecules* **1972**, *5*, 558.
- (14) Flory, P. J. *Macromol. Chem.* **1973**, *8*, 1.
- (15) Flick, J. R.; Petrie, S. E. B. *Bull. Am. Phys. Soc.* **1974**, *19*, 238.
- (16) Yee, A. F. *Ann. N.Y. Acad. Sci.* **1981**, *371*, 341.
- (17) Jones, A. A.; O'Gara, J. F.; Ingfield, P. T.; Bendler, J. T.; Yee, A. F.; Ngai, K. L. *Macromolecules* **1983**, *16*, 658.
- (18) McCammon, J. A.; Lee, C. Y.; Northrup, S. H. *J. Am. Chem. Soc.* **1983**, *105*, 2232.

## Influence of Polydispersity on Polymer Self-Diffusion Measurements by Pulsed Field Gradient Nuclear Magnetic Resonance

P. T. Callaghan\* and D. N. Pinder

Department of Physics and Biophysics, Massey University, Palmerston North, New Zealand. Received June 22, 1984

**ABSTRACT:** The effects of finite polymer polydispersity on the pulsed field gradient nuclear magnetic resonance (PFGNMR) measurement of polymer self-diffusion coefficients is considered both theoretically and experimentally. It is found that polystyrene solutions characterized by a polydispersity  $M_w/M_n < 1.10$  present little difficulty in the interpretation of PFGNMR data. Single-exponential echo decays are observed down to attenuations in excess of 0.05 and the ensemble self-diffusion coefficient obtained lies between  $M_n$  and  $M_w$ . Polymer blends have been studied and the use of deuterated polystyrene has enabled determination of the component self-diffusion coefficients. We observe considerable microscopic averaging of molecular diffusion rates, with the greatest perturbation being suffered by the higher molar mass components. An investigation of the relative importance of reptation and tube renewal as relaxation mechanisms for random coil polymers in semidilute solution reveals that tube renewal is a weak process.

## Introduction

In all experiments dealing with polymer dynamics the influence of finite polydispersity presents a conundrum. In some cases discrepancies are attributed to small polydispersity effects ( $M_w/M_n < 1.10$ ), while in others theories are supported by data obtained where molar mass variations are larger by 1 order of magnitude. A notable ex-

ample of this is the classic self-diffusion study of Klein<sup>1</sup> in which the reptative scaling law  $D \sim M^{-2}$  was exhibited in polyethylene melts whose  $M_w/M_n$  ratios ranged between 1.8 and 3.4.

We have used pulsed field gradient nuclear magnetic resonance (PFGNMR) to measure polymer self-diffusion. It has been recently suggested by von Meerwall<sup>2</sup> on theo-